Modelling shear-flexure interaction in equivalent frame models of slender RC walls

P. E. Mergos
Technological Educational Institute of Chalkida, Greece

K. Beyer
Ecole Polytechnique Fédérale de Lausanne (EPFL), Switzerland

SUMMARY:
Experimental results for quasi-static cyclic tests on reinforced concrete (RC) walls have shown that shear deformations can constitute a significant ratio of the total deformations when the wall is loaded beyond the elastic regime. For walls, which form a stable flexural hinge at their base, the ratio of shear to flexural deformations remains approximately constant over the entire range of imposed displacement ductilities. This is contrary to the common modelling approach of treating the shear deformation as decoupled from the flexural deformations, which leads to constant shear deformations rather than a constant ratio of shear to flexural deformations once a flexural mechanism is formed and the shear force carried by the wall no longer increases. This paper proposes a simplified method of incorporating shear-flexure interaction effect in equivalent frame models of flexure dominated RC walls. In particular, appropriate modifications to the constitutive V-γ law for the wall base section are proposed as a function of the corresponding flexural response. The suggested methodology is implemented in a finite element model consisting of two interacting spread inelasticity sub-elements representing inelastic flexural and shear response. The complete numerical model is incorporated in the general finite element code for damage analysis of RC structures IDARC and it is first validated against experimental results of single RC walls subjected to cyclic loading. In a second step, it is applied in inelastic static and dynamic analyses of a tall wall-frame system. It is shown that ignoring shear-flexure interaction may lead to unsafe predictions in particular regarding seismic demands at the critical ground storey level.

Keywords: Reinforced concrete walls, shear-flexure interaction, seismic analysis

1. INTRODUCTION

Slender capacity-designed RC walls form a stable flexural mechanism when subjected to horizontal loads. In most structural engineering analysis programs the shear stiffness of such walls is assigned a constant value that cannot be updated during the loading process. This modelling approach has been supported by the misconception that the shear deformations will remain constant once the nominal yield force, which is determined by the flexural mechanism, is reached. As a result the ratio of the modelled shear to flexural deformation decreases after the onset of flexural yielding. Experimental evidence, which goes back as far as the 1970s has, however, shown that this does not apply to real RC walls even if the walls are capacity-designed. After flexural yielding the shear deformations continue to increase due to interaction of shear and flexural deformations in the wall's plastic hinge region (Beyer et al. 2011).

Several beam-column element models have been developed to capture shear-flexure interaction in RC members. The most sophisticated fibre elements (displacement or forced based) implement advanced analytical methodologies like the modified compression field theory (e.g. Petrangeli et al. 1998, Guner and Vecchio 2011). However, they necessitate the use of 2D or 3D constitutive material laws and require iterations at each fiber to obtain the section strain field. Hence, the computational effort involved may limit their applicability for response history analysis of complicated multi-storey structures. Other models apply appropriate modifications to phenomenological section V-γ constitutive laws (e.g. Marini and Spacone 2006, Mergos and Kappos 2012) as a function of the

corresponding section flexural demands in terms of curvatures or axial strains. This approach combines both computational efficiency and accuracy.

The analytical models of the latter category have placed emphasis so far on modeling response of RC members with structural deficiencies which fail in shear after yielding in flexure. Application of these models to flexure-controlled RC members has shown that the shear deformations of such members are typically underestimated (Mergos 2009). The objective of this study is therefore to suggest modifications to the base section constitutive V-γ laws of flexure-dominated RC structural walls in order to account for shear-flexure interaction of such members. The suggested modifications are applied to a beam-column element developed previously for the seismic analysis of deficient RC structures (Mergos and Kappos 2009, 2012). The resultant numerical model is first calibrated against experimental data of single slender RC walls. Then, it is implemented in the inelastic analysis of a ten-storey wall-frame RC structure. The necessity of incorporating shear-flexure interaction effect in seismic analysis of tall RC wall-frame systems is revealed.

2. SIMPLE MODELS FOR SHEAR-FLEXURAL INTERACTION IN SLENDER RC WALLS

Results from several series of quasi-static cyclic tests on slender capacity-designed RC walls with different cross sections suggest that the ratio of shear to flexural deformation remains approximately constant over the entire range of applied displacement ductilities. A summary of experimental evidence supporting this hypothesis is presented in Beyer et al. (2011). To illustrate this behaviour, Fig. 2.1 shows the ratios of shear to flexural deformations as a function of the top drift for several cantilever RC walls tested under quasi-static cyclic loading.

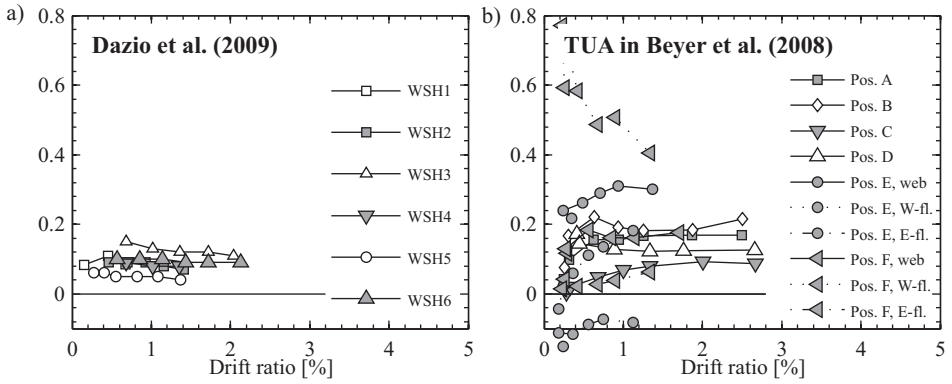

Figure 2.1. Variation of Δ_s/Δ_f ratios with top drift for cantilever RC walls tested under quasi-static cyclic loading (Beyer et al., 2011).

A mechanic's based explanation of this experimental behaviour is provided in Beyer et al. (2011). In this study, by using Mohr's circle and observing that for flexure-dominated RC walls the contributions of horizontal strain in the shear reinforcement and the strain in the compression diagonal to the shear flexibility after flexural yielding may be treated as negligible, Eqn. (2.1) is derived for determining the shear strain γ at the wall base section. In this equation, γ_{fl} is the shear strain due to interaction with flexure, ε_m is the mean axial strain of the wall section, L_w is the length of the wall section, c is the depth of the compression zone, φ the curvature and β a cracking angle representative of the fanned crack pattern (Beyer et al. 2011).

$$\gamma \approx \gamma_{fl} \approx \frac{\varepsilon_m}{\tan\beta} = \frac{\varphi \cdot \left(L_w/2 - c\right)}{\tan\beta} \tag{2.1}$$

By applying this equation and assuming that the shear and flexural deformations outside the plastic hinge region are negligible, Eqn. (2.2) is derived for determining the ratio of shear-to-flexural

displacements Δ_s/Δ_f after flexural yielding. In this equation, H_n is the wall shear span and L_{ph} the plastic hinge length. Given that c remains approximately constant once the section has yielded, Eqn. (2.2) supports experimental evidence indicating that the ratio Δ_s/Δ_f also remains approximately constant over the entire range of applied displacement ductilities (Beyer et al. 2011).

$$\left.\begin{aligned}\Delta_s &\approx \gamma \cdot L_{ph} \approx \frac{\varphi \cdot \left(L_w/2 - c\right) \cdot L_{ph}}{\tan\beta} \\ \Delta_f &\approx \vartheta \cdot H_n \approx \varphi \cdot L_{ph} \cdot H_n\end{aligned}\right\} \rightarrow \frac{\Delta_s}{\Delta_f} = \frac{\left(L_w/2 - c\right)}{H_n \cdot \tan\beta} \tag{2.2}$$

3. BEAM-COLUMN ELEMENT WITH SHEAR-FLEXURE INTERACTION

A beam-column element originally developed for RC column members with sub-standard detailing (Mergos and Kappos 2009, 2012) is applied herein to model shear-flexure interaction in slender RC walls. Finite element components are discussed in the following. Emphasis is placed on the analytical procedures developed to account for shear-flexure interaction in accordance with the observations of the previous section of this study.

3.1. General Formulation

The finite element adopted herein is based on the flexibility approach (force-based element) and belongs to the class of phenomenological models. It consists of two sub-elements representing flexural and shear response (Fig. 1). The two sub-elements are connected in series. Hence, the total flexibility matrix $[F_b]$, relating incremental moments ΔM_A, ΔM_B and rotations $\Delta\theta_A$, $\Delta\theta_B$ at the element flexible ends A and B respectively, is derived by the sum of the flexibility matrices of the flexural $[F_{fl}]$ and the shear $[F_{sh}]$ sub-element.

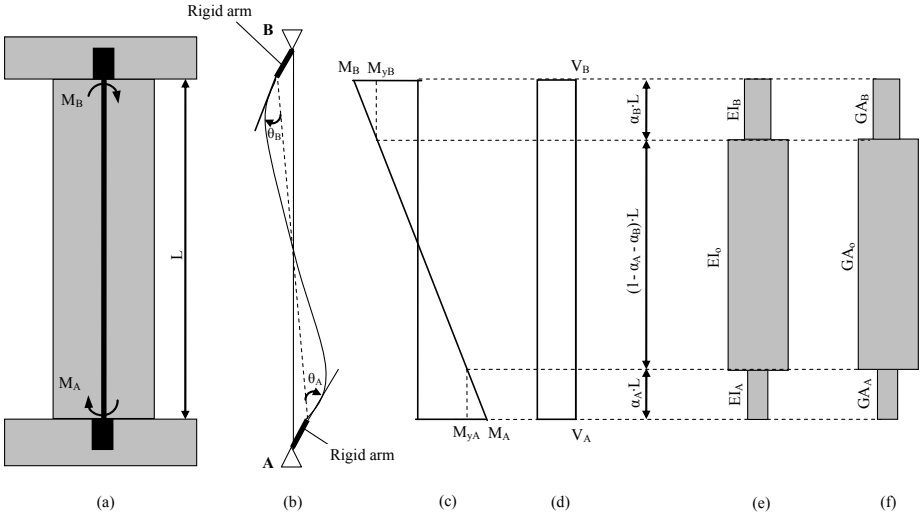

Figure 3.1. Beam-column element with shear-flexure interaction: (a) RC wall; (b) finite element; (c) moment diagram; (d) shear diagram; (e) flexural sub-element; (f) shear sub-element

The flexural sub-element (Fig. 3.1e) is used for modelling flexural behaviour of an RC member before and after yielding of the longitudinal reinforcement. It consists of a set of rules governing the hysteretic moment-curvature (M-φ) response of the member end sections and a spread inelasticity model describing flexural stiffness distribution along the entire member.

The M-φ hysteretic model is composed by the skeleton curve and a set of rules determining response during loading, unloading and reloading. M-φ envelope curve is derived by section analysis and appropriate bilinearization. The Sivaselvan and Reinhorn (1999) hysteretic model, properly modified

to be compatible with a bilinear envelope curve, is adopted to represent M-φ response under cyclic loading. Hysteretic model cyclic degradation parameters are chosen to yield maximum correlation with the respective experimental recordings of five slender RC structural walls tested by Dazio et al. (2009). The obtained values are 4.0 for the unloading stiffness degrading parameter and 0.75 for the slip or crack-closing parameter (Reinhorn et al. 2009).

To capture distribution of section flexural stiffness along the concrete member, a spread inelasticity model is assigned (Soleimani et al. 1979). Following this model, the element is divided into two inelastic end regions and one elastic intermediate zone. Stiffness along the intermediate zone is assumed to be uniform and equal to the elastic stiffness EI_o of the M-φ envelope curve. Flexural stiffness in the inelastic end-zones is defined by the flexural rigidities EI_A and EI_B, which are determined from the M-φ hysteretic relationship of the corresponding end sections (Fig. 3.1e).

In the same figure, α_A and α_B are the yield penetration coefficients. The yield penetration coefficients specify the lengths of the member inelastic zones. In the original formulation of the element (Mergos and Kappos 2009, 2012), these coefficients are determined from the current moment diagram as the part of the element, where acting moment exceeds end section yielding moments M_{yA} and M_{yB}. This formulation represents in a more accurate manner the gradual spread of inelastic deformations from the member ends and it does not require knowledge of moment distribution. However, for cases, where moment distribution is stable and can be predicted with reasonable accuracy, empirical constant values can also be assigned to α_A and α_B like the ones proposed by Priestley et al. (2007) for the equivalent plastic hinge length of RC walls. Having established stiffness distribution along the RC member, the coefficients of the flexibility matrix of the flexural sub-element can be derived by closed form equations determined by the principle of virtual work (Mergos and Kappos 2009, 2012).

In a similar sense, the shear sub-element (Fig. 3.1f) represents the hysteretic shear behaviour of the RC member prior and subsequent to shear cracking and flexural yielding. It consists of a set of rules determining V-γ (shear force vs. shear strain) hysteretic behaviour of the member intermediate and end regions, and a shear spread inelasticity model determining distribution of shear stiffness along the R/C member. Shear hysteresis is determined by the V-γ skeleton curve and a set of rules describing response during unloading and reloading.

In particular, the shear sub-element is divided in two end-zones, where shear-flexure interaction takes place and an intermediate region where interaction with flexure may be disregarded. The lengths of the inelastic end-zones α_A and α_B of the shear sub-element are determined by the respective ones of the flexural sub-element. This formulation assures that shear-flexure interaction effect in slender RC walls is concentrated in the location of the plastic hinges as observed in several experimental studies (Beyer et al. 2011).

Shear stiffness GA_M of the intermediate part of the sub-element is assumed to be uniform and it is determined by the initial V-γ primary curve, without considering shear-flexure interaction effect. The V-γ initial primary curve consists of three branches (Fig. 3.2), but only two different slopes. This approach is adopted in order to distinguish hysteretic shear behaviour before and after flexural yielding as explained in the next section of this study.

The first branch, with uncracked shear stiffness GA_o, connects the origin and the shear cracking point (γ_{cr},V_{cr}), which is defined as the point where the nominal principal tensile stress exceeds the mean tensile strength of concrete (Dazio et al. 2009). The second and third branches of the initial primary curve have the same cracked shear stiffness GA_1 and are separated at the point corresponding to flexural yielding (γ_y,V_y). Shear force corresponding to flexural yielding V_y is determined by equilibrium. Shear strain γ_y is calculated for simplicity by assuming at flexural yielding the same ratio of shear-to-flexural displacements with the one adopted for the whole range of inelastic response.

The stiffness of the inelastic end-zones GA_A and GA_B are defined by the modified V-γ envelope curve (Fig. 3.2), which considers shear-flexure interaction effect as a function of the current maximum

curvature demand of the respective end sections of the flexural sub-element. The methodology for deriving backbone shear stiffness GA_2 after flexural yielding is described in the next section.

To determine shear stiffness at the unloading and reloading stages of response, the hysteretic model of Sivaselvan and Reinhorn (1999) is also adopted herein. However, since shear hysteretic response is characterized by significant pinching and stiffness deterioration, more severe cyclic degradation parameters are applied compared to flexural response. As for flexural hysteretic response, the shear cyclic degradation parameters are chosen to yield best correlation with the respective experimental recordings of five slender RC structural walls tested by Dazio et al. (2009). The derived values are 1.0 for the unloading stiffness degrading parameter and 0.30 for the slip or crack-closing parameter (Reinhorn et al. 2009).

Having established stiffness distribution along the RC member, the coefficients of the flexibility matrix of the shear sub-element are derived by closed form equations determined by the principle of virtual work (Mergos and Kappos 2009, 2012).

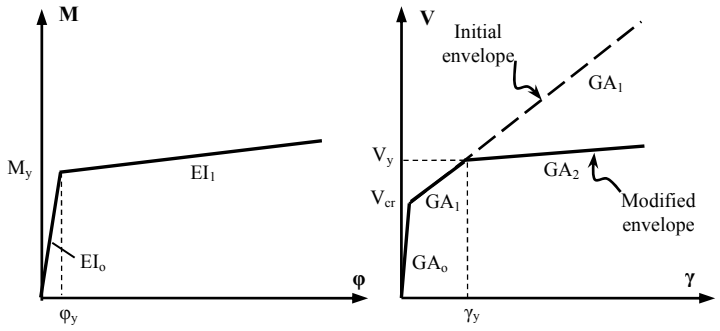

Figure 3.2. End-section envelope curves: (a) M-φ; (b) V-γ

3.2. Determination of tangent envelope shear stiffness in the plastic hinge regions

3.2.1. Walls under general loading conditions

In general, total shear flexibility in the plastic hinge regions after flexural yielding may be considered as the sum of the shear flexibility prior to flexural yielding and the additional shear flexibility induced by shear-flexure interaction effect. Hence, if $\Delta\gamma$ is the total shear strain increment after flexural yielding, $\Delta\gamma_{sh}$ is the shear strain increment due to shear flexibility prior to flexural yielding and $\Delta\gamma_{fl}$ is the shear strain increment developed by interaction with flexure, then

$$\Delta\gamma = \Delta\gamma_{sh} + \Delta\gamma_{fl} \tag{3.1}$$

Shear flexibility prior to flexural yielding is equal to $1/GA_1$ (see Fig. 3.2). If ΔV is the applied shear force increment, then Eqn. (3.2) can be used to determine the shear stiffness GA_2 after yielding in flexure.

$$\Delta\gamma = \Delta\gamma_{sh} + \Delta\gamma_{fl} \rightarrow \frac{\Delta V}{GA_2} = \frac{\Delta V}{GA_1} + \Delta\gamma_{fl} \rightarrow GA_2 = \frac{\Delta V \cdot GA_1}{\Delta V + \Delta\gamma_{fl} \cdot GA_1} \tag{3.2}$$

Shear strain increment developed by interaction with flexure $\Delta\gamma_{fl}$ can be calculated by Eqn. (3.3) as described in the previous section of this study. This equation implies a linear variation of γ_{fl} with φ, if c is assumed constant after flexural yielding. This assumption is typically adequate. However, variation of c can easily be taken into account by the proposed analytical procedure (see Fig. 3.3).

$$\Delta\gamma_{fl} = \left(L_w / 2 - c\right) \cdot \Delta\varphi / \tan\beta \tag{3.3}$$

Equations (3.2) and (3.3) provide current tangent shear stiffness GA_2 as a function of GA_1, ΔV and $\Delta\varphi$. Hence, GA_2 can be considered as independent of the wall loading conditions since it is based on local responses. No assumptions regarding moment distribution are required. However, GA_2 also affects ΔV and $\Delta\varphi$ since it influences the flexibility matrix of the element. Hence, an iterative analytical scheme should be assigned, which terminates when GA_2 converges with a pre-specified tolerance.

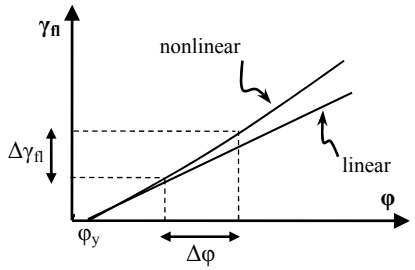

Figure 3.3. Variation of $\gamma_{,fl}$ with curvature demand

Furthermore, for the vast majority of flexure dominated RC walls developing inelastic response, the shear flexibility prior to flexural yielding $1/GA_1$ may be disregarded since it represents a negligible fraction of the total shear response (Beyer et al. 2011). By applying this simplification and substituting Eqn. (3.3) in Eqn. (3.2), the following equation can be used for determining GA_2.

$$GA_2 = \frac{\Delta V}{\Delta\gamma_{fl}} = \frac{\Delta V}{\left(L_w/2 - c\right)\cdot\Delta\varphi/\tan\beta} \tag{3.4}$$

3.2.2. Cantilever walls

In this section, it is shown how for the special case of cantilever walls, Eqn. (3.4) can be further simplified. For cantilever walls, the shear force increment ΔV can be written as $\Delta M/H_n$. Hence, Eqn. (3.4) becomes

$$GA_2 = \frac{\Delta M}{H_n\cdot\left(L_w/2 - c\right)\cdot\Delta\varphi/\tan\beta} \tag{3.5}$$

After flexural yielding, the ratio $\Delta M/\Delta\varphi$ represents the post-yielding M-φ envelope flexural tangent stiffness EI_1 (see Fig. 3.2). By this substitution, Eqn. (3.6) is derived.

$$GA_2 = \frac{EI_1}{H_n\cdot\left(L_w/2 - c\right)/\tan\beta} \tag{3.6}$$

Eqn. (3.6) is important because it shows that for slender cantilever RC walls a constant tangent envelope shear stiffness value $GA_2<GA_1$ may be assigned in the plastic hinge regions after flexural yielding when modeling shear-flexure interaction. This holds under the general assumption that the neutral axis depth remains constant after yielding in flexure. Otherwise, an average value for c could be applied with reasonable accuracy.

It is important to remember that Eqn. (3.6) should be applied only in the particular cases, where the point of contra-flexure is known and remains constant throughout structural response. Otherwise, it may yield significant errors in the prediction of inelastic shear deformations. Equation (3.6) may also be rewritten as a function of the shear-to-flexural displacements Δ_s/Δ_f ratio, which has been shown (Beyer et al. 2011) to be approximately independent of the imposed ductility demand. By proper substitution of Eqn. (2.2) in Eqn. (3.6), the following equation is derived:

$$GA_2 = \frac{EI_1}{\left(\frac{\Delta_s}{\Delta_f}\right) \cdot H_n^2} \tag{3.7}$$

4. VALIDATION AGAINST EXPERIMENTAL RESULTS OF A CANTILEVER RC WALL

The proposed numerical model is fully implemented in the general finite element code IDARC2D developed at the State University of New York at Buffalo (Reinhorn et al. 2009). In this section, it is validated against the experimental results of a single RC wall specimen subjected to quasi-static cyclic loading.

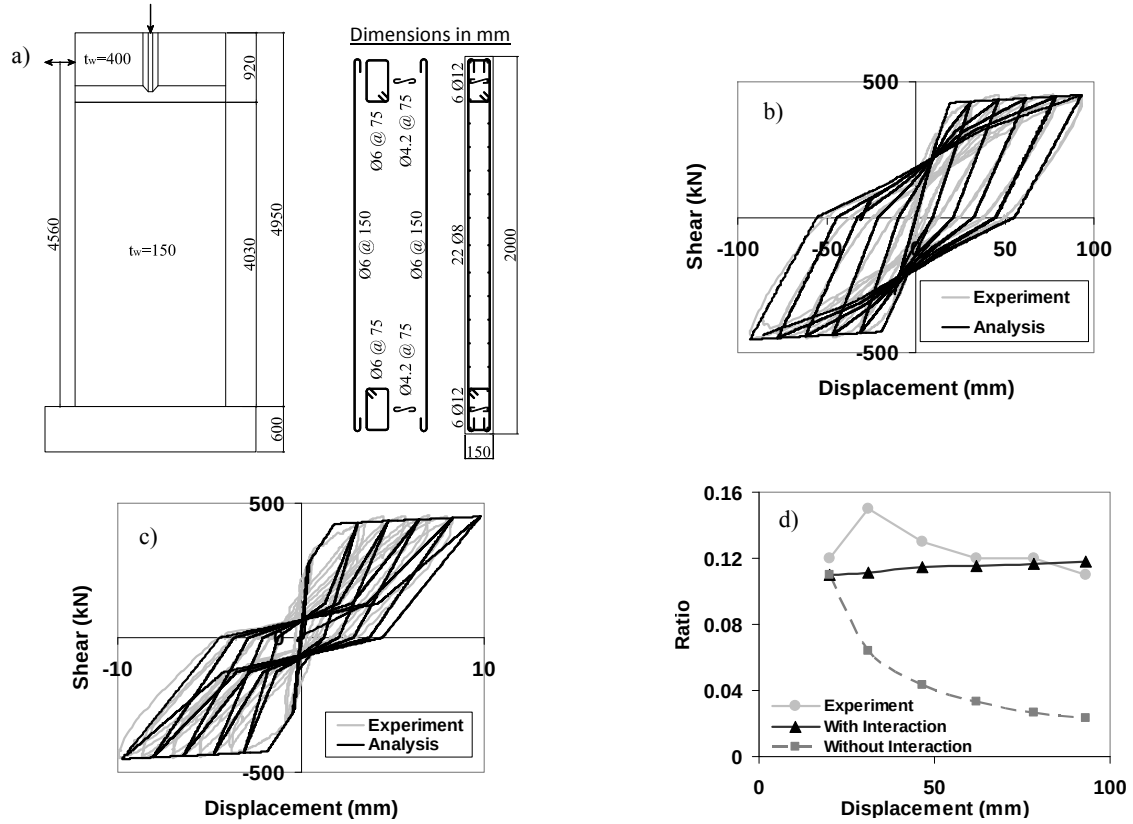

Figure 4.1. RC structural wall WSH3 by Dazio et al. (2009): (a) structural configuration; (b) shear force vs. total displacement; (c) shear force vs. shear displacement; (d) variation of shear-to-flexural displacement ratio with imposed top displacement demand

Dazio et al. (2009) performed quasi-static cyclic tests on six RC walls at the ETH Zurich. The main scope was to investigate the effect of different vertical reinforcement contents and different reinforcement ductility properties, typical for Central Europe, on the deformation behaviour of slender RC walls. Herein, the RC wall specimen WSH3 (Fig. 4.1a) is examined. The test unit was 2.00m long and 0.15m wide. The length of the shear span was 4.56m. During cyclic loading, the specimen was subjected to a constant compressive axial load equal to 686kN. Details on reinforcement configuration and material properties can be found in Dazio et al. (2009).

For the analysis of the specific specimen, a single finite element is applied. The length of the inelastic end-zones is assumed constant and equal to the plastic hinge length proposed for RC walls by Priestley et al. (2007). In this manner, anchorage slip effect is, indirectly, taken also into consideration. Both Eqn. (3.4) and (3.6) were applied for the determination of GA_2. These equations were found to yield identical results. Angle β is estimated by the equation proposed by Collins and Mitchell (1997).

Figure 4.1b presents lateral load vs. lateral displacement response as derived by the proposed model and as recorded experimentally. It can be seen that the analytical model reproduces with sufficient accuracy the experimental initial stiffness, lateral load capacity, unloading and reloading stiffness.

Furthermore, Fig. 4.1c presents a comparison of the predicted and the recorded lateral top displacement developed by shear deformations. In this figure, it is clear that experimental shear displacements increase considerably after flexural yielding and they contribute a considerable part of the total response. Adequate prediction of the magnitude of inelastic shear displacements is achieved by the shear-flexure interaction analytical procedures described in this study. It is worth noting that shear hysteresis is characterized by significant pinching and unloading stiffness deterioration. These phenomena are well captured by the proposed model. The above show that the finite element follows closely not only total, but also individual component displacement response.

Figure 4.1d illustrates the variation of the shear-to-flexure displacement ratio with the imposed top displacement demand. It can be inferred that the experimental ratio remains approximately constant throughout the loading history. This is well represented by the analytical model proposed in this study. On the other hand, if interaction with flexure is neglected, then the same ratio is grossly underestimated as the level of inelasticity increases. It is worth noting that, even when modeling shear-flexure interaction, Δ_s/Δ_f does remain exactly constant as inelasticity progresses. This is due to the influence of the flexural and shear deformations outside the plastic hinge region. However, it is clear that this deviation is insignificant and may be disregarded in the analytical procedure.

5. ANALYSIS OF A WALL-FRAME STRUCTURE

Shear-flexure interaction effect is examined in a ten-storey wall-frame structure designed according to a previous version of EC8 for ductility class ‘M’. Concrete and steel classes are C20/25 and S400 respectively. Soil category is ‘A’. Frame geometry is presented in Fig. 5.1a. Analytical design of the specific frame is described in Penelis and Kappos (1997).

Three different finite element models are applied for the seismic analysis of this frame. Model 1 includes only flexural deformations. Model 2 accounts for flexural and shear deformations without considering their interaction. Finally, Model 3 takes into consideration the interaction of shear and flexural flexibilities. Since wall moment distribution varies throughout structural response, Eqn. (3.2) is applied for GA_2 determination accompanied by the necessary iterative scheme. Furthermore, the length of the inelastic zone at the base of the wall is defined by the current moment diagram following the gradual spread plasticity approach (see Fig. 3.1) as described in Mergos and Kappos (2012). The main scope of this section is to investigate if and how slender wall shear-flexure interaction modifies the distribution of damage for tall wall-frame structures.

Figures 5.1 and 5.2 present the main results of pushover analysis until onset of lateral failure, which is assumed herein to coincide with onset of flexural failure at the base of the RC wall. Figure 5.1b shows that shear-flexure interaction has only a negligible effect on the global lateral stiffness of the wall-frame structure. However, shear flexure interaction increases by approximately 10% the top displacement capacity of the wall-frame system.

Figure 5.1c reveals an important resultant of shear-flexure interaction in the plastic hinge region of the slender RC walls. In this figure, distribution of normalized interstorey drifts at a top displacement corresponding to an average drift of 2% is presented. The figure shows that the normalized drift of the base storey increases by approximately 30%, when interaction is taken into account. This is due to the increase of inelastic shear deformations in the plastic hinge region when shear-flexure interaction is taken into account. Unlike flexural displacements, which increase gradually over the height, inelastic shear displacements are concentrated in the locations of the plastic hinge regions.

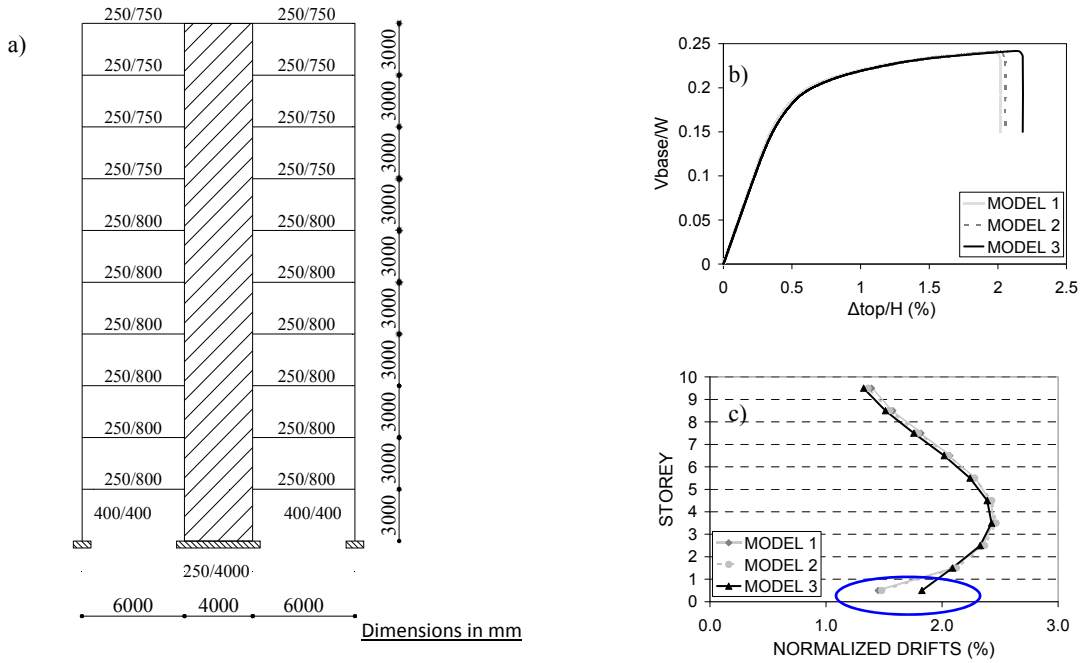

Figure 5.1. (a) Geometry of the wall-frame structure; (b) pushover base shear over weight vs. top displacement over total height; (c) maximum normalized interstorey drifts from pushover analysis at 2% top displacement

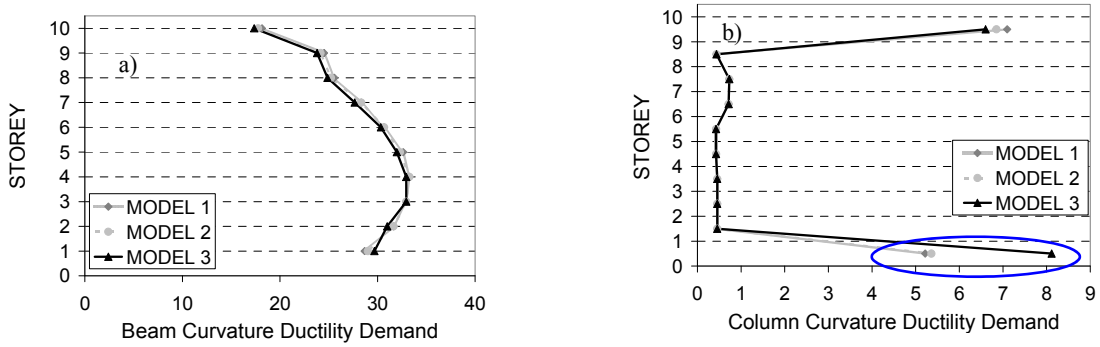

Figure 5.2. Pushover analysis maximum curvature ductility demands at a top displacement corresponding to an average drift of 2%: (a) beams; (b) columns

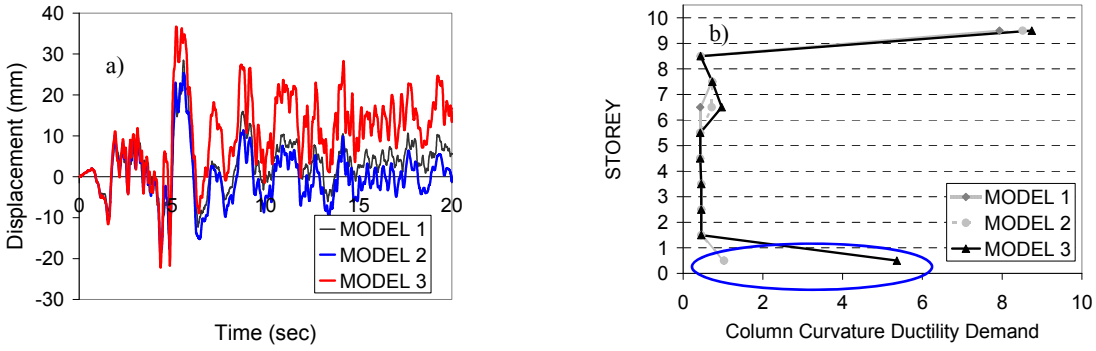

Figure 5.3. Time history analysis results: (a) 1st storey displacement response; (b) maximum column curvature ductility demands

Figure 5.2a illustrates the distribution of maximum developed beam curvature ductility demands at a top displacement corresponding to an average drift of 2%. The results show that shear-flexure interaction has a insignificant influence on beam damage distribution. Last, Fig. 5.2b presents distribution of column maximum curvature ductility demands for the same top displacement. Shear-

flexure interaction leads to a significant increase in the inelastic deformation demand of the base column. This increase is related to the larger interstorey drift at the base and may adversely affect the integrity of the frame when not accounted for in design.

Finally, Fig. 5.3 illustrates the basic time history analysis results of this frame for the El-Centro 1940 N-S ground motion record. A higher PGA value of 0.5g is applied in order to obtain significant damage for the frame under investigation. In general, the same conclusions can be drawn with pushover analysis. Fig. 5.3a presents the 1st storey time history responses. It is evident that shear-flexure interaction leads to an important increase in the peak and residual storey displacements. The concentration of inelastic deformations at the base level leads to the significant increase of the base column curvature ductilitydemands (Fig. 5.3b). In particular, the column curvature demand rises from 1.1 to 5.4, when modeling properly inelastic shear wall response.

6. CONCLUSIONS

A simplified methodology is presented for incorporating shear-flexure interaction of slender walls in seismic analysis of RC structures. Building on mechanics and experimental evidence, appropriate modifications are proposed to the phenomenological wall base section constitutive V-γ law. The modifications are implemented in a distributed inelasticity beam-column element incorporated in a general finite element framework. The numerical outcome is first validated against experimental recordings of a single slender RC wall. It is then employed in the seismic analysis of a tall wall-frame structure. Comparing pushover and time-history analysis results of models which neglect or consider shear-flexure interaction, underlines the importance of including shear-flexure interaction for slender RC walls when analysing wall-frame structures.

REFERENCES

Beyer, K., Dazio, A. and Priestley, M.J.N. (2008). Quasi-static cyclic tests of two U-shaped reinforced concrete walls. *Journal of Earthquake Engineering* **12:7**, 1023-1053.

Beyer, K., Dazio, A. and Priestley, M.J.N. (2011). Shear deformations of slender RC walls under seismic loading. *ACI Structural Journal* **108:2**, 167-177.

Collins, M.P. and Mitchell, D. (1997). Prestressed Concrete Structures, Response Publications, Toronto, ON, Canada.

Dazio, A., Beyer, K. and Bachmann, H. (2009). Quasi-static cyclic tests and plastic hinge analysis of RC structural walls. *Engineering Structures* **31**, 1556-1571.

Guner, S. and Vecchio, F.J. (2010). Pushover analysis of shear-critical frames: formulation. *ACI Structural Journal* **107:1**, 63-71.

Marini, A. and Spacone, E. (2006). Analysis of reinforced concrete elements including shear effects. *ACI Structural Journal* **103:5**, 645-655.

Mergos, P.E. and Kappos, A.J. (2009). Modelling Gradual Spread of Inelastic Flexural, Shear and Bond-slip Deformations and their Interaction in Plastic Hinge Regions of R/C Members. *Second COMPDYN Conference*, Rhodes, Greece.

Mergos, P.E. and Kappos, A.J. (2012). Seismic Damage Analysis of RC Structures with Substandard Detailing, Computational Methods in Earthquake Engineering Vol. 2, Springer (In Press).

Penelis, G.G., Kappos, A.J. (1997). Earthquake-resistant Concrete Structures, E & FN SPON (Chapman & Hall), London.

Petrangeli, M., Pinto, P. and Ciampi, V. (1999). Fibre element for cyclic bending and shear or R/C structures. I: Theory. *Journal of Engineering Mechanics* **125:9**, 994-1001.

Priestley, M.J.N., Calvi, G.M. and Kowalsky, M.J. (2007). Displacement-Based Seismic Design of Structures. IUSS Press, Pavia, Italy.

Reinhorn, A.M, Roh, H., Sivaselvan, M. et al. (2009). IDARC2D Version 7.0: A Program for the Inelastic Damage Analysis of Buildings. Report MCEER-09-0006, University at Buffalo, State Univ. of New York.

Sivaselvan, M.V. and Reinhorn, A.M. (1999). Hysteretic Model for Cyclic Behaviour of Deteriorating Inelastic Structures. Report MCEER-99-0018, University at Buffalo, State Univ. of New York

Soleimani, D., Popov, E.P. and Bertero, V.V. (1979). Nonlinear Beam Model for R/C Frame Analysis. *Seventh Conference on Electronic Computation*. St. Louis, Misouri.